Does β-PbO$_2$ harbor topological states?

Sharad Mahatara and Boris Kiefer ⓘ

Department of Physics, New Mexico State University, Las Cruces, NM 88003, United States of America

E-mail: bkiefer@nmsu.edu

Abstract

The electronic properties of β-PbO$_2$, have been controversial for several decades. Experiments find behavior ranging from metallic, attributed to oxygen vacancies, to indirect semiconducting for stoichiometric samples with a gap of 0.61 eV. Theory leads to similar ambiguities, and predicts this phase to be metallic (PBE, HSE06) or to possess a small bandgap (HSE06). An area where this inconsistency is amplified, is when a material behavior depends on the electronic structure in the vicinity of the Fermi energy, such as topological states. In our work, we use a self-consistent DFT $+$ U approach and find that stoichiometric β-PbO$_2$ to be an indirect semiconductor with a band gap of ∼0.8 eV, similar to experiment. The larger bandgap requires at least ∼4% strain, to drive β-PbO$_2$ into a nodal line semimetallic state, significantly larger strains than reported previously. Moreover, we find that the nodal line semimetallic state is not protected against spin-orbit-coupling. Also, the surface computations do not show any evidence for topologically protected states near the Fermi energy. Therefore, our results strongly suggest that β-PbO$_2$ is a topologically trivial material, consistent with experiment, but in stark contrast to previous computations. Previously reported topologically protected states in β-PbO$_2$ are attributed to an inaccurate description of the (bulk) optical properties.

Keywords: density-functional-theory, self-consistent Hubbard-U, optical bandgap, topological materials

1. Introduction

Metal dioxides (MO$_2$) continue to attract significant scientific and technological interest. Depending on the nature of the metal, they find a wide range of technological applications. For example, MO$_2$ (M = Hf and Zr) oxides have emerged as attractive gate dielectric materials due to their stability, large dielectric constant and wide bandgap [1], while SnO$_2$ is beneficial for solar cells due to its long-term stability and high carrier mobility [2]. β-PbO$_2$ which crystallizes in the rutile structure, has been widely used as electrode material in the lead-acid batteries for over a century [3]. Yet, the optical and electronic properties of β-PbO$_2$ are not well-understood. Previous experiments show that sub-stoichiometric β-PbO$_2$ is metallic [4–6] due to oxygen vacancies. Another study showed that stoichiometric β-PbO$_2$ is an n-type semiconductor with carrier concentration of ∼10^{19} to 10^{23} cm^{-3} and an indirect bandgap of 0.61 eV [7].

Previous density functional theory (DFT) calculations showed semimetallic character for β-PbO$_2$, with overlap of valence and conduction band at the Γ-point [8, 9]. In contrast, HSE06 calculations reported that this material is a semimetal [10–12], or a direct semiconductor with a bandgap of only ∼0.08 eV with a valance band maximum (VBM) at the Γ-point [2], or an indirect semiconductor with the VBM at the R-point, [13], consistent with experiment [7], albeit with an underestimated bandgap of ∼0.23 eV.

An area where this inconsistency of electronic structure is amplified, is when a material property depends on the electronic structure in the vicinity of the Fermi level, such as topological states of matter [12, 14–17]. More recently, β-PbO$_2$ has attracted renewed interests [10–12] with the emergence of topological semimetals [16–18]. Topological semimetals are stabilized by non-trivial band crossing points in the Brillouin zone, and classified as 3D Dirac semimetal (DSM) [16], Weyl semimetal (WSM) [17], and nodal-line semimetal (NLSM) [18]. In some cases, (i.e. reference [14]) spin–orbit-coupling (SOC) opens a gap transforming a nodal-line semimetal into a topological insulator (TI) [19]. In general rutile oxide (space group $P4_2/mnm$) can support two distinct types of the nodal lines [20]: (1) the nodal line (NL) is in the (110) or ($\bar{1}$10) planes, which are topologically protected by mirror symmetry and SOC opens a gap between the otherwise degenerate Dirac points; and (2) the NL remains

Table 1. Previous works on topological states in β-PbO$_2$. Note: 0% strain corresponds to equilibrium.

	Bandgap (eV)	Method	Condition (strain%)	SOC
NLSM	0.08	HSE06 [2]	1	No
NLSM	0	HSE06 [10]	0	Yes
DSM	0	HSE06 [12]	0	Yes
TI	0	PBE [14]	0	Yes

Table 2. Crystal and electronic data for β-PbO$_2$ calculated by using PBE and ACBN0 functional and compared to HSE06 functional and the experiment. The lattice parameters: a and c are given in Å. E_g^{ind} is the indirect bandgap (in eV) between Γ- and R-points.

	PBE	ACBN0	HSEO6	Exp.
		This work	[13]	[7]
a	4.8786	4.9240	4.9602	4.9509
c	3.3330	3.3569	3.3759	3.3830
E_g^{ind}	—	0.82	0.23	0.61
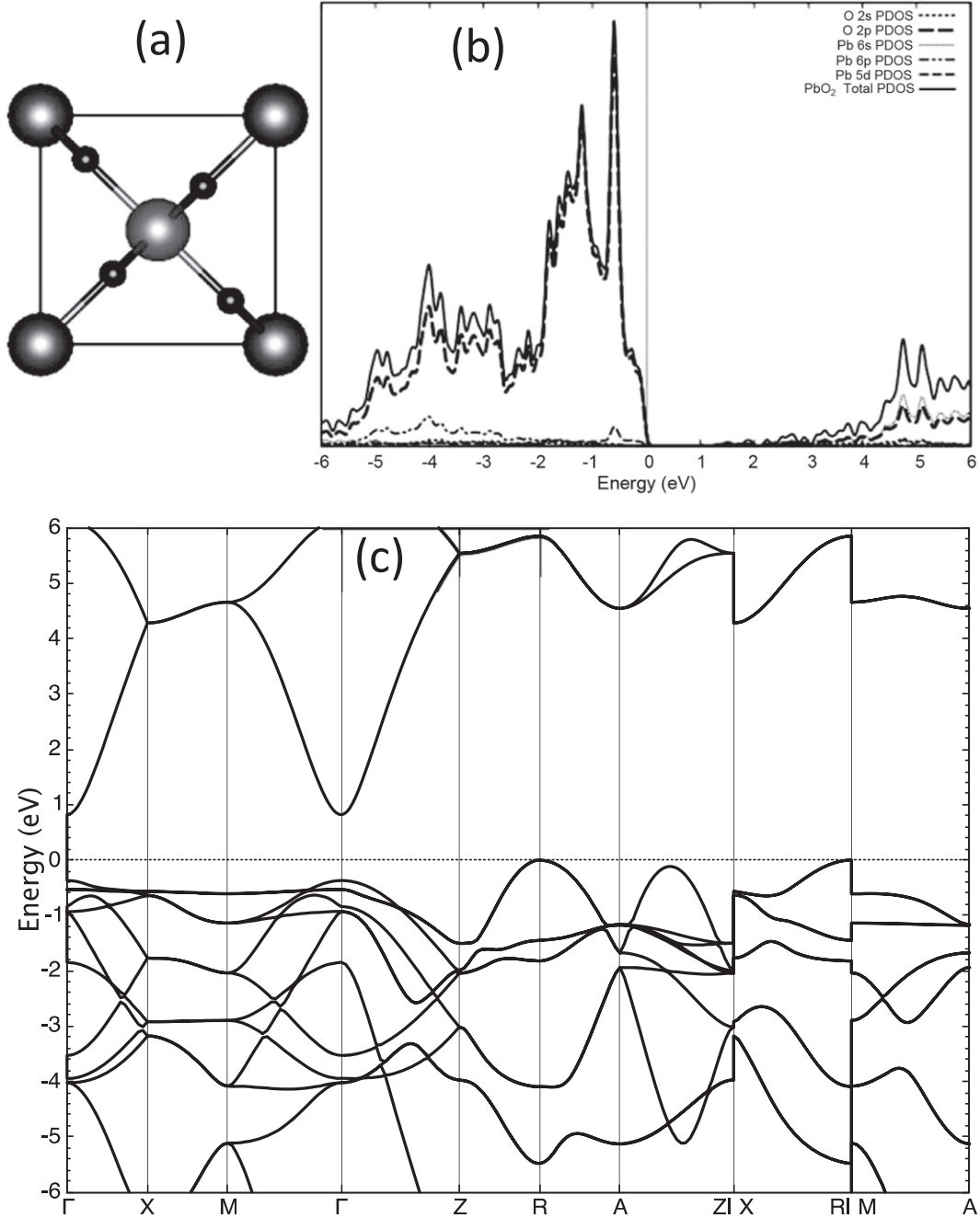
Figure 1. (a) β-PbO$_2$ viewed along [001] direction, (b) ACBNO calculated total and partial density of states (PDOS) of β-PbO$_2$, and (c) equilibrium bandstructure of β-PbO$_2$ calculated with ACBN0 functional [23]. The Brillouin zone path selection follows AFLOW scheme [28].
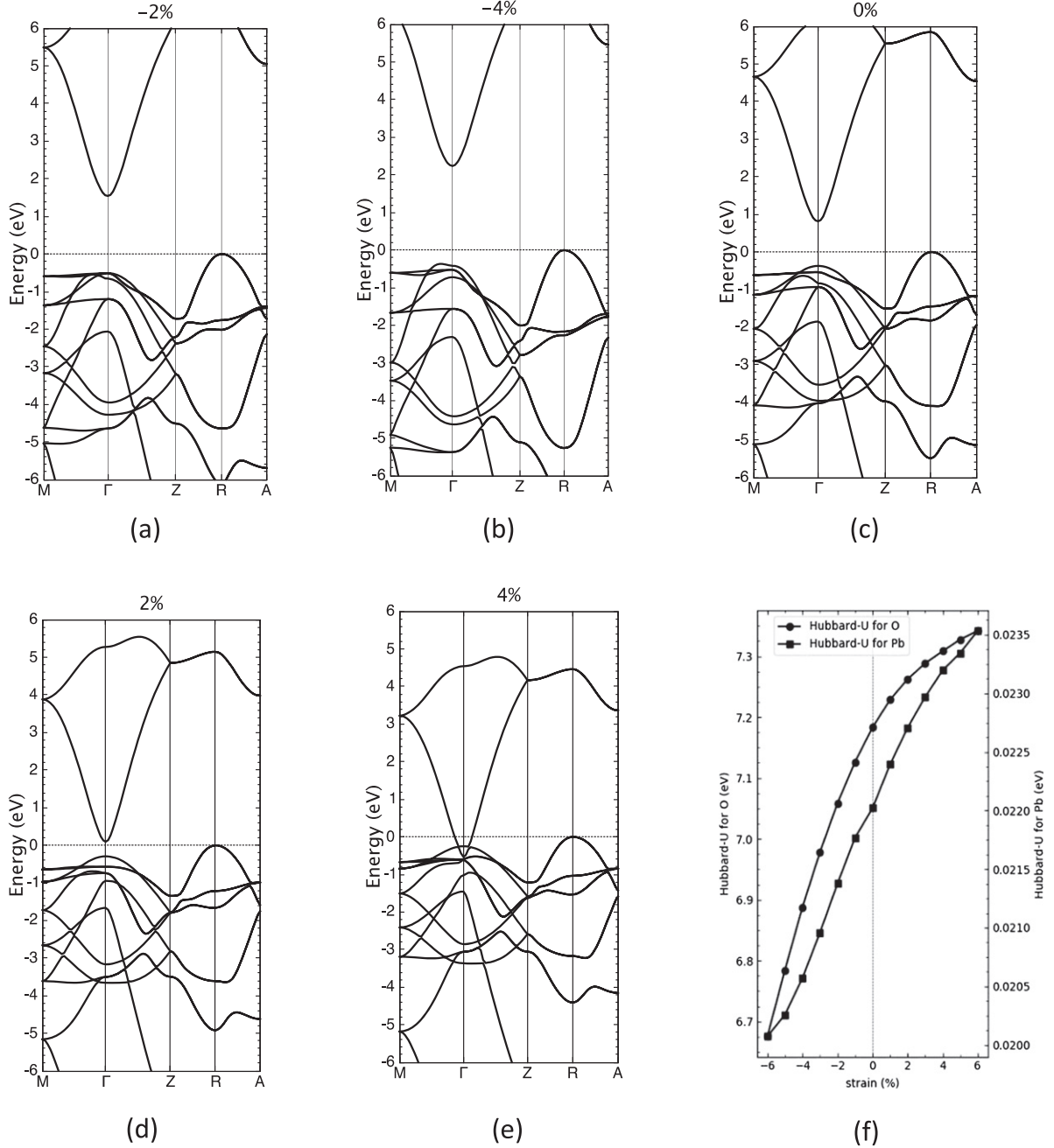
Figure 2. Strain dependence of the electronic structure in β-PbO$_2$ for strain components $\varepsilon_{11} = \varepsilon_{22} = \epsilon$, $\varepsilon_{33} = 2\epsilon$, (a) $\varepsilon = -2\%$, (b) $\varepsilon = -4\%$, (c) equilibrium, $\varepsilon = 0\%$, (d) $\varepsilon = +2\%$, (e) $\varepsilon = +4\%$, (f) strain dependence of self-consistent Hubbard-U.

degenerate even in the presence of SOC as shown for example in isostructural IrO$_2$ [21]. In this case, states at the Fermi level are protected by non-symmomorphic symmetry operations.

As a result, β-PbO$_2$ has been predicted to be a three-dimensional topological semimetal under a variety of different conditions (table 1), including equilibrium [10, 12], a low temperature phase transition [11], or applied strain [2], and incompatible topological properties in the presence of SOC: DSM [12], NLSM [2, 10], and TI [14]. SOC assists in stabilizing topological states in β-PbO$_2$, especially if VBM and conduction band minimum (CBM) energy differences are underestimated, and/or fundamental optical properties such as the indirect/direct band gap are not sufficiently well captured.

In most of these previous studies, topological properties originated from the predicted semimetallic electronic state of β-PbO$_2$ at equilibrium (table 1).

In this contribution, we use a self-consistent DFT + U approach, that has been successful for correcting optical properties in transition metal oxides [22]. We use the ACBN0 strategy [23, 24], to determine self-consistent Hubbard-U values using Quantum Espresso [25]. We employed ultrasoft pseudopotentials from the pslibrary 1.0 database [26], and the PBE exchange correlation functional [27]. All computations were preformed using a plane wave cutoff for energy and density of 90 Ry and 900 Ry, respectively. Monkhorst–Pack $4 \times 4 \times 6$ and $6 \times 6 \times 1$ k-point grids were used for the bulk

calculations, and surface calculations, respectively. All crystallographic degrees of freedom were relaxed to reach the static ground state, with and without SOC. Atomic positions were relaxed in all computations, but the volume was only relaxed in the bulk simulations. The (001) surface was modeled as slabs of various thicknesses, that are separated by a vacuum perpendicular to the surface of at least 5-unit cells (>15 Å). Starting from the strained configurations all atomic positions were optimized while the strained lattice remained fixed.

2. Results and discussion

The ACBN0 functional was applied to β-PbO$_2$ to study its electronic properties. Our computed effective Hubbard-U values at equilibrium are $U_{Pb} = 0.022$ eV, and $U_O = 7.18$ eV, for Pb and O, respectively. These values are very similar to those we computed for isostructural TiO$_2$: $U_{Ti} = 0.19$ eV and U_O (2p) = 7.0 eV. Moreover, the Hubbard-U for β-TiO$_2$ are in very good agreement with previous work (reference [23]): $U_{Ti} = 0.15$ eV and U_O (2p) = 7.34 eV. PBE underestimates the lattice parameters by $\sim$1.4% compared to experiment, while ACBN0 improves the comparison with experiment and underestimates the lattice constants by only $\sim$0.5% (table 2). Analysis of the ACBN0 calculated total and partial density of states (PDOS), figure 1(b), shows that the VBM is dominated by O 2p states, consistent with the expected large charge transfer from Pb to O. The CBM in contrast shows Pb 6s and O 2p states as expected. The band structure (figure 1(c)) shows that the VBM is located at the R-point, consistent with experiment [7], the bandgap in the ACBN0 computations is higher than the experimental value by $\sim$0.2 eV (figure 1(c) and table 2). The ACBN0 valence band structure agrees with a previous HSE06 calculation [13], with the only difference that the ACBN0 bandgap is larger (table 2).

3. Strain-induced phase transition in β-PbO$_2$

In materials like β-PbO$_2$ when SOC is neglected, band inversions occur at one or more high symmetry points in the Brillouin zone, resulting in two doubly degenerate bands crossing each other to form a fourfold degenerate nodal line [2, 10, 12]. This situation is realized in β-PbO$_2$ with PBE computations [12] and HSE06 computations [10, 12] where band-crossing at the VBM located at the Γ-point are predicted. Previous work, [2] based on HSE06 calculations found β-PbO$_2$ to be a trivial insulator ($E_g \sim 0.08$ eV) at zero pressure transforming to an NLSM phase by applying a hydrostatic tensile strain of 1%. Our ACBN0 computed indirect bandgap is $\sim$10 times larger, the VBM is at the R-point rather than the Γ-point. Consequently, we find that a significantly higher hydrostatic tensile strain, $\sim$6%, is needed to drive β-PbO$_2$ into a gapless semimetallic state. Thus, our results suggest that previous computations significantly overestimated the potential of β-PbO$_2$ to show a band-inverted gapless state for reasonable strain magnitudes. Volume conserving strain, akin to the approximate volume conservation due to interface formation showed no band inversion at least up to 6%
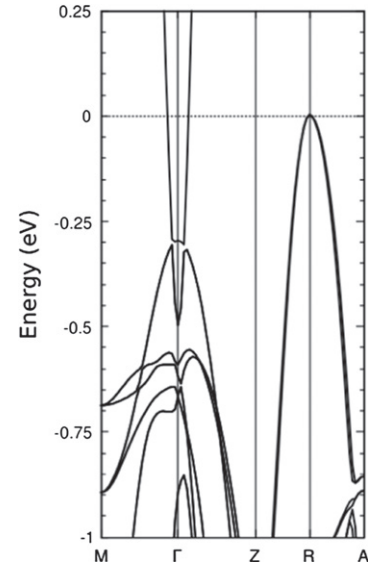

Figure 3. ACBN0 + SOC bulk bandstructure for β-PbO$_2$ with asymmetric strain of $\varepsilon = 4$%.

strain. In order to investigate if other strains exist that lower the strain magnitude to reach bandgap closure, we considered an asymmetric strain with $\varepsilon_{xx} = \varepsilon_{yy} = \varepsilon \neq 0$ within the basal plane and $\varepsilon_{zz} = 2\varepsilon$ along the c-axis, where ε are $\pm$2% and $\pm$4%. For positive tensile strain, both the basal plane and the z-direction expand, but by different amounts. We have investigated the effect of these asymmetric strains on the bandstructure of β-PbO$_2$ for strains ranging from $\varepsilon = -4$% to $\varepsilon = +4$% (figure 2). For strains below $\varepsilon = +2$%, β-PbO$_2$ is an indirect semiconductor (figures 2(a)–(c)). At strain higher than $\varepsilon = +2$%, the bandgap closes at the Γ-point (figure 2(d)). As the strain is increased further, band inversion occurs and a semimetallic state is reached for strain of $\sim$4% along the basal plane (figure 2(e)). This strain, while still large, is significantly smaller in magnitude as compared to a hydrostatic tensile strain (6%) and a volume conserving strain ($>$6%), which could facilitate its realization for example at an interface. While our findings are qualitatively similar to previous work [2], however, in contrast to this previous study with VBM at the Γ-point, our computed VBM is at the R-point. Therefore, occupied electronic states at the Γ-point are below the Fermi level and higher strains are needed to reach band inversion, as compared to the case where VBM and CBM are both at the Γ-point. However, similar to previous work two Dirac points emerge along the M–Γ and Γ–Z direction in momentum space, the hallmark of NLSMs (figure 2(e)).

We observe a total variation of Hubbard-U parameter between -6% to 6% strain of $\sim$17% and $\sim$12% for Pb and O, respectively. In our calculation, 4% strain is required to obtain band inversion (figure 2(e)). If we fix the Hubbard-U values at their equilibrium values, we find a band gap of $E_g \sim 0.8$ eV, and a smaller strain of $\sim$3% is sufficient to obtain band inversion, consistent with the smaller Hubbard-U (figure 2(f)). Therefore, qualitatively similar results are obtained for computations with the equilibrium Hubbard-U, or a strain re-optmized Hubbard-U.
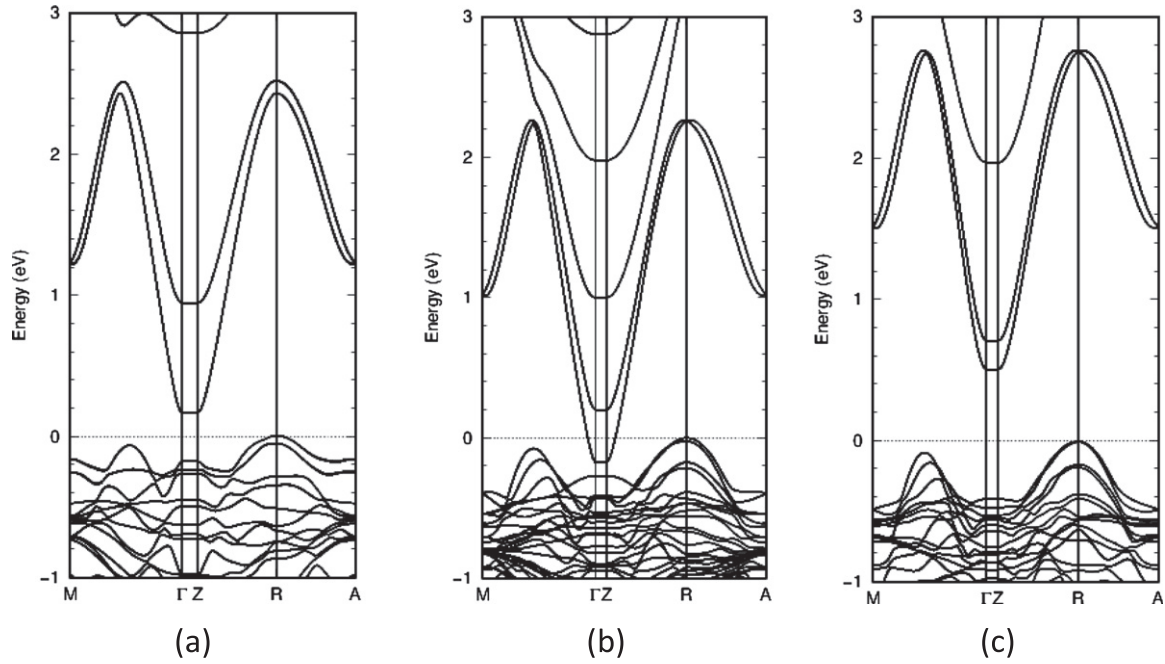
Figure 4. (001)-surface states in β-PbO$_2$ with SOC: (a) $\varepsilon = 4\%$, 2-unit cells thick slab, (b) $\varepsilon = 4\%$, 5-unit cells thick slab, (c) equilibrium, 5-unit cells thick slab.

4. Topological nodal line states in β-PbO$_2$?

For the computation in the presence of SOC for 4% asymmetric strain (figure 3), the Hubbard-U parameters were used for the corresponding strain (Pb = 0.023 eV and O = 7.30 eV, figure 2(f)). Even when SOC is taken into account, the band structures are almost identical, with the important caveat, that a small SOC induced gap ($\sim$1 meV) opens along M–Γ and Γ–Z direction (figure 3). This observation is identical to reference [14], where SOC turns an NLSM β-PbO$_2$ into a small gap TI. However, the gapped states are below the Fermi level and β-PbO$_2$ remains metallic.

Creating a surface is a well-known method to investigate topological states [29]. We computed the electronic structure for the (001) surface obtained from the $\varepsilon = 4\%$ asymmetrically strained bulk (figure 2e) in order to identify the character of the nodal line. The relaxation of the (001) surface reduces the strain along the c-axis from the initial $\varepsilon_{zz} = 8\%$ to less than $\sim$0.8%. In contrast, the strain was maintained in the (x,y)-plane, due to the fixed lattice and the extended bond network in this plane. Both ACBN0 and ACBN0 + SOC showed the same behavior. In the absence of SOC, we find that the bandgap decreases from $\sim$0.15 eV for a 2-unit cells thick slab, to a metallic state for slab-thicknesses for 3-, 4-, and 5-unit cells, similar to a previous report for TlBiTe$_2$ and TiBiSe$_2$ [29]. For 2-unit cells thick slabs (figure 4(a)), β-PbO$_2$ is semiconducting with and without SOC. However, if SOC is included 3-, 4-, and 5-unit cells thick slabs show a gapped surface state below the Fermi level and unaffected flat bands along the Γ–Z direction (figure 4(b)). The gapped surface states of β-PbO$_2$ indicate a topologically trivial material. Our (001) surface computations including SOC for equilibrium β-PbO$_2$ for a 5-unit cells thick slab also shows a topologically trivial semiconducting state (figure 4(c)). In summary, the surface computations show no evidence for topologically protected states near the Fermi energy. Therefore, our results show that in contrast to previous computations β-PbO$_2$ is a topologically trivial material, consistent with experiment. The uncertainty of the topological character of β-PbO$_2$ in previous studies is attributed to the inaccurate description of the optical properties of the bulk.

5. Conclusions

The self-consistent Hubbard-U computations of β-PbO$_2$ reported here predict the VBM to be at the R-point, and the CBM to be at the Γ-point, with an indirect band gap of E_g $\sim$ 0.8 eV, consistent with experiment. We find that Hubbard-U values increase systematically with increasing strain from $\varepsilon = -6\%$ to $\varepsilon = +6\%$ in β-PbO$_2$, with a total variation of $\sim$12% for O and $\sim$17% for Pb. With the application of $\varepsilon = +4\%$ tensile strain along the basal plane and $\varepsilon = 8\%$ along the c-axis, using the self-consistent Hubbard-U, β-PbO$_2$ transforms into an NLSM. The strains reported here are significantly higher than reported previously and attributed to the underestimated bandgap in previous studies. Using the equilibrium Hubbard-U, instead of the strain-optimized Hubbard-U, we find an NLSM state for a slightly smaller strain of $\varepsilon = 3\%$, due to a decreased bandgap, but still, significantly higher than previously reported. In contrast to previous studies that characterized β-PbO$_2$ as a topologically non-trivial material, we find that the NLSM state is not protected against SOC. Our surface calculations show that β-PbO$_2$ does not host any topologically protected states near the Fermi energy. Therefore, in contrast to previous studies, we find β-PbO$_2$ to be a topologically trivial material. The differences in the topological characterization are attributed to the insufficiently well resolved

electronic, and optical properties in bulk β-PbO$_2$ in previous works.

ORCID iDs

Boris Kiefer ⓘ https://orcid.org/0000-0003-0242-3165

References

[1] Wang B, Huang W, Chi L, Al-Hashimi M, Marks T J and Facchetti A 2018 High-k gate dielectrics for emerging flexible and stretchable electronics *Chem. Rev.* **118** 5690–754

[2] Ma F, Jiao Y, Gao G, Gu Y, Bilic A, Sanvito S and Du A 2016 Substantial band-gap tuning and a strain-controlled semiconductor to gapless/band-inverted semimetal transition in rutile lead/stannic dioxide *ACS Appl. Mater. Interfaces* **8** 25667–73

[3] Planté G 1860 C.R. Hebd. Seances *Acad. Sci.* **50** 640 http://gallica.bnf.fr/ark:/12148/bpt6k3007r.image

[4] Piette L H and Weaver H E 1958 NMR Chemical Shifts of Pb207 in a Few Compounds *J. Chem. Phys.* **28** 735–6

[5] Frey D A and Weaver H E 1960 NMR Measurements of the Knight Shift in Conducting PbO2 *J. Electrochem. Soc.* **107** 930–2

[6] Pohl J P and Schlechtriemen G L 1984 Concentration, mobility and thermodynamic behaviour of the quasi-free electrons in lead dioxide *J. Appl. Electrochem.* **14** 521–31

[7] Payne D J, Paolicelli G, Offi F, Panaccione G, Lacovig P, Beamson G, Fondacaro A, Monaco G, Vanko G and Egdell R G 2009 A study of core and valence levels in β-PbO2 by hard X-ray photoemission *J. Electron Spectrosc. Relat. Phenom.* **169** 26–34

[8] Payne D J, Egdell R G, Hao W, Foord J S, Walsh A and Watson G W 2005 Why is lead dioxide metallic? *Chem. Phys. Lett.* **411** 181–5

[9] Heinemann M, Terpstra H J, Haas C and De Groot R A 1995 Electronic structure of β-PbO 2 and its relation with BaPbO 3 *Phys. Rev.* B **52** 11740

[10] Zhang R W, Liu C C, Ma D S, Wang M and Yao Y 2018 Nodal-line semimetal states in the positive-electrode material of a lead-acid battery: Lead dioxide family and its derivatives *Phys. Rev.* B **98** 035144

[11] Chen T, Shao D, Lu P, Wang X, Wu J, Sun J and Xing D 2018 Anharmonic effect driven topological phase transition in Pb O 2 predicted by first-principles calculations *Phys. Rev.* B **98** 144105

[12] Wang W, Deng L, Jiao N, Zhou P and Sun L 2017 Three-Dimensional Dirac Semimetal β-PbO2 *Phys. Status Solidi* **11** 1700271

[13] Scanlon D O, Kehoe A B, Watson G W, Jones M O, David W I, Payne D J, Egdell R G, Edwards P P and Walsh A 2011 Nature of the band gap and origin of the conductivity of PbO 2 revealed by theory and experiment *Phys. Rev. Lett.* **107** 246402

[14] Wang Z and Wang G 2017 A new strongly topological node-line semimetal β-PbO2 *Phys. Lett.* A **381** 2856–9

[15] Wehling T O, Black-Schaffer A M and Balatsky A V 2014 Dirac materials *Adv. Phys.* **63** 1–76

[16] Wang Z, Sun Y, Chen X Q, Franchini C, Xu G, Weng H, Dai X and Fang Z 2012 Dirac semimetal and topological phase transitions in A 3 Bi (A= Na, K, Rb) *Phys. Rev.* B **85** 195320

[17] Wan X, Turner A M, Vishwanath A and Savrasov S Y 2011 Topological semimetal and Fermi-arc surface states in the electronic structure of pyrochlore iridates *Phys. Rev.* B **83** 205101

[18] Burkov A A, Hook M D and Balents L 2011 Topological nodal semimetals *Phys. Rev.* B **84** 235126

[19] Hasan M Z and Kane C L 2010 Colloquium: topological insulators *Rev. Mod. Phys.* **82** 3045

[20] Yang S Y, Yang H, Derunova E, Parkin S S, Yan B and Ali M N 2018 Symmetry demanded topological nodal-line materials *Adv. Phys.: X* **3** 1414631

[21] Lin J J, Huang S M, Lin Y H, Lee T C, Liu H, Zhang X X, Chen R S and Huang Y S 2004 Low temperature electrical transport properties of RuO2 and IrO2 single crystals *J. Phys.: Condens. Matter* **16** 8035

[22] Park S G, Magyari-Köpe B and Nishi Y 2010 Electronic correlation effects in reduced rutile TiO 2 within the LDA+ U method *Phys. Rev.* B **82** 115109

[23] Agapito L A, Curtarolo S and Nardelli M B 2015 Reformulation of DFT+ U as a pseudohybrid hubbard density functional for accelerated materials discovery *Phys. Rev.* X **5** 011006

[24] Supka A R, Lyons T E, Liyanage L, D'Amico P, Al Orabi R A R, Mahatara S, Gopal P, Toher C, Ceresoli D, Calzolari A and Curtarolo S 2017 AFLOWπ: A minimalist approach to high-throughput *ab initio* calculations including the generation of tight-binding hamiltonians *Comput. Mater. Sci.* **136** 76–84

[25] Giannozzi P, Baroni S, Bonini N, Calandra M, Car R, Cavazzoni C, Ceresoli D, Chiarotti G L, Cococcioni M, Dabo I and Dal Corso A 2009 QUANTUM ESPRESSO: a modular and open-source software project for quantum simulations of materials *J. Phys.: Condens. Matter* **21** 395502

[26] Garrity K F, Bennett J W, Rabe K M and Vanderbilt D 2014 Pseudopotentials for high-throughput DFT calculations *Comput. Mater. Sci.* **81** 446–52

[27] Perdew J P, Burke K and Ernzerhof M 1998 Perdew, burke, and ernzerhof reply *Phys. Rev. Lett.* **80** 891

[28] Setyawan W and Curtarolo S 2010 High-throughput electronic band structure calculations: Challenges and tools *Comput. Mater. Sci.* **49** 299–312

[29] Eremeev S V, Bihlmayer G, Vergniory M, Koroteev Y M, Menshchikova T V, Henk J, Ernst A and Chulkov E V 2011 *Ab initio* electronic structure of thallium-based topological insulators *Phys. Rev.* B **83** 205129